**Article:**
Zheng, J, Gao, L, Zhang, H et al. (5 more authors) (2021) eICIC configuration of Downlink and Uplink Decoupling with SWIPT in 5G Dense IoT HetNets. IEEE Transactions on Wireless Communications, 20 (12). pp. 8274-8287. ISSN 1536-1276

https://doi.org/10.1109/TWC.2021.3091639

# eICIC configuration of Downlink and Uplink Decoupling with SWIPT in 5G Dense IoT HetNets

Jie Zheng, Ling Gao, Haijun Zhang, *Senior Member, IEEE*, Dusit Niyato, *Fellow, IEEE*, Jie Ren, Hai Wang, Hongbo Guo, Zheng Wang

***Abstract*—Interference management and power transfer can provide a significant improvement over the 5th generation mobile networks (5G) dense Internet of Things (IoT) heterogeneous networks (HetNets). In this paper, we present a novel approach to simultaneously manage inferences at the downlink (DL) and uplink (UL), and to identify opportunities for power transfer and additional UL transmissions integrated with existing protocols and infrastructures for enhanced inter-cell interference coordination (eICIC) protocol in dense IoT HetNets, while considering practical non-linear energy harvesting (EH) model. The design is formulated as the joint optimization of interference aware UL/DL decoupling, airtime resource allocation and energy transfer. The key insight of our algorithm is to translate the original, intractable joint-optimization problem into a problem space where a good approximate solution can be quickly found. We evaluate our scheme through theoretical analysis and simulation. The evaluation shows that our approach improves the system utility by over 20% compared to start-of-the-art in dense IoT HetNets. Compared to alternative schemes, our approach maintains the best user fairness and rate experience and can solve the problem in a fast and scalable way.**

***Index Terms*—Downlink/Uplink decoupling (DUDe), Enhanced inter-cell interference coordination (eICIC), Simultaneous wireless information and power transfer (SWIPT), Internet of Things (IoT), heterogeneous network (HetNet).**

## I. Introduction

By deploying different network infrastructures, such as macrocells and dense deployment of smallcells (e.g.,picocell or femtocell), the dense Internet of Things (IoT) heterogeneous network (HetNet) is widely seen as a solution for the 5th generation mobile networks (5G) [1]. Unlike human-based cellular devices, such as smart phones, that can be charged easily, these massive IoT devices are usually very difficult to charge or replace their batteries. This has led to an increasing interest in energy-efficient communication of IoT devices from the system design. While there has been considerable work on optimizing downlink (DL) performance [2] [3] [4], emerging Machine Type Communication (MTC), and other upload-intensive applications such as sensing information of large-scale IoT devices make uplink (UL) performance just as important.

Meanwhile, there is no consensus on how to make the best use of the heterogeneous infrastructures within a dense IoT HetNet. Since smallcells typically share the frequency band with macrocell, the performance of a low-power smallcell could be severly impacted by the interference from high-power macrocell. The 3rd Generation Partnership Project (3GPP) has proposed the notion of enhanced inter-cell interference coordination (eICIC) to protect the DL smallcell transmissions by mitigating the interference from neighboring macrocells, which keeps silent for certain periods, termed Almost Blank Subframes (ABS) [2].

However, how to set the eICIC parameters, i.e., ABS subframes configuration and DL association (smallcell range expansion expand bias (REB) or smallcell selection bias (CBS)), is left unspecified in eICIC standard. There has been considerable work on the eICIC configuration, such as Fixed ABS [5] [6], Dynamic ABS [2] [3], Dynamic ABS with DUDe [4], UM-ABS with DUDe [7].

- *Fixed ABS*: This strategy uses the fixed eICIC configuration, and sets the fixed ABS, and sets the fixed REB for each smallcell [5] [6]. In [5] [6], they don't consider the dynamic configuration of eICIC.
- *Dynamic ABS*: The dynamic ABS configuration is to allocate ABS, and to determine the flexible DL association rules with REB based on the optimization problem of eICIC configuration [2] [3], which only focus on the DL transmission.
- *Dynamic ABS with DUDe*: With considering the DL/UL Decoupling (DUDe), this is the dynamic ABS with DUDe joint optimization approach for user equipment (UE) associations under dynamic Time-division Duplex (TDD), and it assumes that the UL and DL could be splitted to the different BSs [4].
- *UM-ABS with DUDe*: This is UM-ABS with DUDe, which exploits the UL transmission for macrocells in ABSs for dynamic eICIC configuration in HetNets [7], referred to UM-ABS, to improve the system performance.

This work was supported in part by the National Natural Science Foundation of China (Grants nos. 61701400, 62072362, 61822104, 61771044), by International Science and Technology Cooperation Project of Shannxi(2020KW-006), the Fundamental Research Funds for the Central Universities(FRF-TP-19-002C1, RC1631), Beijing Top Discipline for Artificial Intelligent Science and Engineering, University of Science and Technology Beijing.

J. Zheng, L. Gao, Hai Wang and Hongbo Guo are with State-Province Joint Engineering and Research Center of Advanced Networking and Intelligent Information Services, School of Information Science and Technology, Northwest University, Xian, 710127, Shaanxi, China.(jzheng@nwu.edu.cn, gl@nwu.edu.cn, hwang@nwu.edu.cn and guohb@nwu.edu.cn)

H. Zhang is with Institute of Artificial Intelligence, Beijing Advanced Innovation Center for Materials Genome Engineering, Beijing Engineering and Technology Research Center for Convergence Networks and Ubiquitous Services, University of Science and Technology Beijing, Beijing 100083, China (e-mail: haijunzhang@ieee.org).

D.Niyato is with Nanyang Technological University, Singapore.(dniyato@ntu.edu.sg)

J. Ren is with Shaanxi Normal University, China.(renjie@snnu.edu.cn)

Z. Wang is with University of Leeds, United Kingdom.(z.wang5@leeds.ac.uk)

Recently, simultaneous wireless information and power transfer (SWIPT) technology is gaining tremendous attention due to its ability in providing sustainable and ubiquitous communications for numerous wireless communication scenarios, including IoT [8]. Therefore, we design a novel eICIC configuration with SWIPT for IoT dense HetNets. We propose to configure energy transfer splitting of DL during nABSs with DUDe for UL transmission which takes into eICIC with considering the UL transmission for macro during ABSs (UM-ABS) in dense IoT HetNets, termed DL energy power transfer UM-ABS (DPT-UM-ABS). Our approach can improve the energy problem for IoT, while carrying out the interference coordination between macrocell and smallcell to improve the system rate, especially for the UL rate of IoT UE.

From the perspective of communication, the application of SWIPT to IoT devices essentially focuses on the optimal tradeoff between the system rate and the harvested energy which is usually solved by computational optimization. This paper aims to push the boundary of computational optimization by simultaneously considering DL/UL decoupling (DUDe), resource allocations and energy transfer. Doing so can lead to better ABS utilization of SWIPT to dense IoT HetNet. A key challenge is how to quickly explore the extremely large design space to find a suitable optimization configuration at an affordable cost. Our key insight is that the highly complex optimization space can be mapped and tailored down to a smaller problem space by using a set of heuristics, where the alternating direction method of multipliers (ADMM) [9] – a robust and efficient method for solving large-scale, distributed optimization problems – can then employed to derive a good solution in a faster and scalable manner.

We demonstrate how our approach can be integrated with the existing eICIC under the TDD paradigm to minimize the disruptions for deployment. We evaluate our approach by applying it to typical dense IoT HetNet scenarios through simulations, and we analytically prove that our approach has a low computation complexity. Experimental results show that our approach improves the system utility by over 20% compared to state-of-the-art methods [2], [4], [7] that specifically target ultra-dense network optimizations, delivering 94% of the up-bound performance (found through exhaustively searching all possible parameter settings). We show that our approach not only provides the best network-wide system utility, but also maintains the most robust and the highest standard of proportional fairness and user experience (measured by user-received rates) among all competitive schemes.

The main contributions of this paper can be summarized as follows:

- First, we propose to configure energy transfer splitting of DL with practical SWIPT during nABSs with DUDe which takes into eICIC with considering UM-ABS for eICIC in dense IoT HetNets, especially the IoT devices have a non-linear energy harvesting (EH) model for practical SWIPT.
- Second, we jointly optimize DUDe UE-associations, resource allocation of UE, dynamic DPT-UM-ABS allocation between macrocell and smallcell and energy transfer splitting for UL and DL in dense IoT HetNets, which can be modelled as a general form consensus problem with regularization effectively solved by ADMM;
- Final, we employ the ADMM-based algorithm to solve the joint-optimization problem by decomposition-coordination procedure, which is transformed into an equivalent consensus formulation with separable objectives for macrocell and smallcell. Then the local optimization subproblems can be solved by proposing a two-step iterative scheme with dynamic programming based algorithms and the auxiliary variable transferred convex algorithm, which can be carried out in the distributed manner.

## II. Related work

The resource allocation of joint DL and UL in HetNet receives considerable interests in the recent years. Shen *et al.* [10] show that it can be profitable to dynamically configure the DL and UL in a HetNet of TD-LTE. Nikolaos *et al.* [4] study joint $\alpha$-fair optimization of user association and TDD allocation. The [11] studies the joint DL and UL traffic offloading under asymmetric information for CSI. Taking all possible TDD subframes configuration, coupled and decoupled cell associations strategies are investigated based on a geometric probability approach [12]. The [13] focuses on optimizing the average UL-DL per user Degrees of Freedom with considering a backhaul constraint. The joint scheme with DUDe, multiple region frequency allocation, convergent power control under non-uniform user distribution is proposed to improve the performance of UL [14]. Finally, our work aims to maximize the utility of network's capacity to improve rate and fairness of user. It can benefit from other complementary works on energy optimization [15], D2D [16], or quality of services [17].

The recent work presented in [18] has exploited the property of channel reciprocity to develop resource allocation schemes for SWIPT for single-tier networks. Kishk *et al.* [19] study joint UL and DL coverage of cellular-based ambient RF energy harvesting IoT in the single-tier cellular network. However, both prior approaches do not consider the multi-tier HetNets where the cross-tier interference is non-negligible. An energy efficiency (EE) optimized strategy based on eICIC technology is proposed by taking into account the user assocation, ABS ratio, resource allocation in the frequency domain, and the power transmission of the macro BSs, but without considering the UL transmission [20]. It has found that resource allocation with a practical non-linear EH model can achieve larger rate-energy region than the linear EH model for SWIPT [21] [22]. The [23] investigates the energy efficiency (EE) maximization problem of non-orthogonal multiple-access (NOMA) with non-linear EH model SWIPT in HetNets. As a departure from prior work, our approach considers the dynamic eICIC configuration problem of non-linear EH SWIPT and cross-tier interference for UL and DL in dense IoT HetNets. For future, our work can be extend with NOMA Network with imperfect CSI [24], intelligent reflecting surface-aided coordinated multipoint [25] and the mobile edge computing with fairness [26] in dense IoT HetNets.

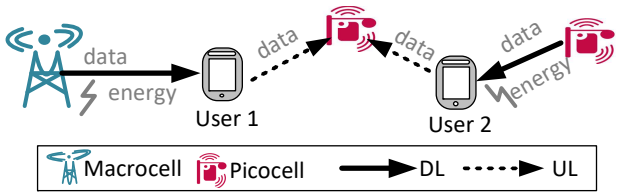


Figure 1. Overview of our network model. We consider a two-tier HetNet that consists of macro and pico cells where a user's UL and DL can be associated with different cells.

Table I
LIST OF PARAMETERS AND NOTATIONS USED IN THE PAPER

| Parameter | Description |
|---|---|
| $u \in U$ | A user, $u$, in a set of users, $U$ |
| $m \in M$ | A macrocell, $m$, from a set of macrocells, $M$ |
| $s \in S$ | A smallcell, $s$, from a set of smallcells, $S$ |
| $i$ | The index of a BS, where $i \in M \cup S$ |
| $v_{BS}$ | The range expansion bias BS ($m$ or $s$) in the DL |
| $F$ | The number of subframes for one period of ABS |
| $A_s$ | The number of ABS subframes for small BS, $s$ |
| $B_m$ | The number of nABS subframes for macro BS, $m$ |
| $c^{UL}_{u,A}$ | The allocated resource for ABS from macrocell $m$ on the UL |
| $d^{UL}_{u,A}$ | The allocated resource for ABS from smallcell $s$ on the UL |
| $c^{UL}_{u,nA}$ | The allocated resource for nABSs from macrocell $m$ on the UL |
| $d^{UL}_{u,nA}$ | The allocated resource for nABSs from smallcell $s$ on the UL |
| $c^{DL}_{u,nA}$ | The allocated resource for nABSs from macrocell $m$ on the DL |
| $d^{DL}_{u,nA}$ | The allocated resource for nABSs from smallcell $s$ on the DL |
| $P^{Rx}_u$ | The received power of user equipment (UE) $u$ |
| $P^{DL}_m$ | The transmitting power of macrocell $m$ on the DL |
| $P^{DL}_s$ | The transmitting power of smallcell $s$ on the DL |
| $P^{UL}_u$ | The transmitting power of user $u$ from UE $u$ on the UL |
| $I_{m(s)}$ | The interference set suffer from macrocell (smallcell) |
| $I_u$ | The set of users that interfere with user, $u$ (UE-to-UE) |
| $H_{u,u}$ | The channel gain for different two users |
| $H_{u,BS}$ | The channel gain between user and BS, BS $\in \{m, s\}$ |
| $H_{BS,BS}$ | The channel gain for different BS, BS $\in \{m, s\}$ |

## III. SYSTEM MODEL

In this work, we consider a two-tier HetNet consisting of macrocell and smallcell, and target dynamic TDD where the UL/DL subframes for users can be dynamically allocated. As depicted in Figure 1, we use SWIPT in the DL transmission so that a user can first harvest the energy in the DL and then uses it for UL transmission. The UL and DL can access to different BS e.g. MBS or SBS in Figure 2. UL and DL with SWIPT leverages eICIC so that it can be easily integrated with existing protocols and infrastructures. As is shown in Figure 3, we allow UL transmissions to a macrocell within an ABS (UM-ABS) [7] and identify opportunities for transferring energy during nABSs and ABSs. Furthermore, to add clarity, Table I gives the frequently used parameters of the paper.

### A. Problem Scope

Our work aims to improve the overall network performance by considering three optimization strategies: interference-aware UL/DL decoupling, airtime resource allocation and energy transfer in ultra-dense HetNets. We focus on improving radio access but not backhaul because DUDe does not impose a tight requirement on the backhaul capacity [27]. For performance evaluation, we consider three network-wide metrics: (1) the system utility, (2) the average UL, DL and overall rates across users, and (3) the proportional fairness. These metrics are defined in Section VII-A.

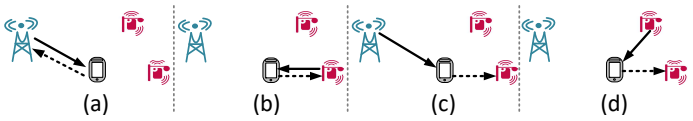


Figure 2. The four user association modes considered in this work.

### B. Asymmetric Association Models

*User association:* We consider four association modes in a HetNet, as illustrated in Figure 2. The first two modes (a and b in Figure 2) are when the UL and DL of a UE are associated with the same type of cell (macrocell or smallcell). The other two modes are when the UL and DL are associated with two cells (c and d in Figure 2) where the UL is associated with a smallcell and the DL can be associated with a macrocell or a smallcell. Allowing the DL and UL to be associated with different cells enable us to use heterogenous cells to better distribute the traffic loads, which is particularly attractive for cell edge users.

*DL association:* The DL of a UE can be associated with either a macrocell or a smallcell in HetNets. If the DL of a UE chooses to associate a suitable cell with maximum received signal strength traditionally, this strategy leads to overloading a macrocell and by underutilizing the densely deployed smallcells. To offload the DL traffic from an MBS to a SBS, we associate a UE according to a configurable BS selection bias factor, $v_{BS}$, between the MBS and the SBS. Specifically, a UE can associate with a BS by considering the reference signal received power (RSRP), $RSRP_{u,BS}$ between the UE and a BS (i.e., a macrocell or smallcell) in the whole bandwidth. This goal is defined as:

$$UE^{DL} = argmax \{RSRP_{u,BS} + v_{BS}\} \quad (1)$$

There are scenarios where the DL of a cell-edged UE can be associated with either an MBS or a SBS (see Section III-B). The determine the cell assignment, we firstly calculate the difference of the RSRP between the candidate MBS and SBS [3]. The difference, $\epsilon_u$, is calculated as $\epsilon_u = RSRP^{DL}_{u,m} - RSRP^{DL}_{u,s}$, where $RSRP^{DL}_{u,m}$ and $RSRP^{DL}_{u,s}$ are the RSRP (measured by the UE) of the MBS and SBS, respectively. Then, we look at the range expansion bias (REB), $v_s$. We assign UEs with a $\epsilon_u$ value that is smaller than the REB to a smallcell, and the remaining to a macrocell.

In practice, the REB is determined on an MBS-SBS pair basis. Because a smallcell typically defines the minimum adjustment for changing the REB, we use this setting to map the range of possible REB values to a set of discrete integers between zero and the total number of candidate UEs that can be associated with the target smallcell $s$. Here, the total number of candidate UEs is denoted as $\nu^{max}_s$. In the boundary cases where the REB takes 0 or $\nu^{max}_s$, all candidate UEs will be assigned to a SBS or MBS cell respectively.

*UL association:* Unlike the DL, performing power control on the UL has little benefit for interference management in an ultra-dense cellular network due to the short distance between the UE and a cell. Therefore, we assume the UE uses the maximum transmit power and associates with a cell (macro or

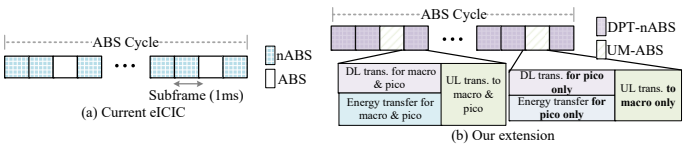


Figure 3. Our approach extends the current eICIC (a) for UL transmission during ABS subframes and energy transfer during subframes (b).

pico) that gives the strongest signal power. Note that utilizing power control on UL to improve the cell's energy efficiency is out of the scope of this work.

An asymmetric UL/DL association scheme might associate a UE with different cells or BSs. This means the scheme might associate a UE with a nearby SBS in the UL, even the UE is associated with the MBS in the DL, because doing so gives a better channel gain. To model the composite channel gain from a UE to a BS, the UL association of UE $u$ is decided by:

$$UE^{UL} = argmin\ \{H_{u,BS}\} \tag{2}$$

where $H_{u,BS}$ is the channel gain of the association – which includes the path-loss, shadowing, and fading. We maximize the rate gain by minimizing $H_{u,BS}$.

### C. Resource Allocation Modeling and Extensions

eICIC was introduced in LTE R10 to support inference management in HetNets using the ABS. As depicted in Figure 3(a), the idea is to keep the macrocells periodically silent (by only transferring reference signals with reduced power) to allow smallcells to send information to UEs with little interference during an ABS (i.e., an ABS time slice).

*Resource modeling:* Suppose an ABS cycle of $F$ subframes in TDD has $A_s$ ABSs and $B_m$ nABSs, where $B_m$ nABSs is the number of subframes transmitted by MBS $m$ and $A_s$ ABSs is the number of subframes transmitted by SBS $s$. It is clear that $A_s$ ABSs and $B_m$ nABSs must be an integer because we cannot further divide a subframe. Because an UE can occupy the entire bandwidth, we can extend the subchannel or subcarrier allocation. Our work can be extended to the OFDM for HetNets. For example, the total available subchannels or subcarriers are $N$ for one subframe, so the total available $NF$ an ABS cycle, and $NA_s$ ABSs and $NB_m$ nABSs.

*Our extensions:* As depicted in Figure 3(b), we utilize an ABS cycle in two ways. Firstly, we allow UL transmissions to a macrocell within an ABS to improve the network throughput [7]. Secondly, we identify opportunities for transferring energy during nABSs and ABSs (the latter was not exploited in prior work). We refer the first strategy as UM-ABS (UL transmission in ABSs) and the latter as DPT-nABS (DL power splitting in nABSs). We jointly consider the UM-ABS and DPT-nABS for eICIC in dense IoT HetNets, termed DPT-UM-ABS.

### D. The Energy Harvesting Model

The received power of UE $u$ from the associating BS is:

$$P_u^{Rx} = p_{BS}^{DL} \cdot H_{u,BS} + p_u^{Int} \tag{3}$$

where $p_{BS}^{DL} \cdot H_{u,BS}$ is the useful signal, $p_u^{Int}$ is the average inter-cell interference measured by the UE, $p_{BS}^{DL}$ is the transmitting power of BS ($m$ or $s$) in the DL.

Using this formula, the rate received by a UE is obtained from a fraction of the received power $\rho_u P_u^{Rx}$, $\rho_u$ is the power splitting ratio that is allocated for information processing for the UE [22]. The input power at the energy harvest receiver UE is $P_u^{IN} = (1-\rho_u)P_u^{Rx}$, where $1-\rho_u$ is the energy splitting ratio for energy harvest given by the target user. It has been found that the energy conversion efficiency with traditional linear EH model is irrelevant to the input power at the EH receiver [21] [23]. Therefore, we adopt a practical parametric non-linear EH model based on the logistic (sigmoidal) function which captures the dynamics of the RF energy conversion efficiency for different input power levels [21]. The harvested energy at UE $u$, $P_u^{UL}$, can be modelled as:

$$\begin{aligned} P_u^{UL} &= \frac{\Psi_u - M_u\Omega_u}{1-\Omega_u}, \Omega_u = \frac{1}{1+exp(a_u b_u)}, \\ \Psi_u &= \frac{M_u}{1+exp(-a_u(P_u^{IN}-b_u))}. \end{aligned} \tag{4}$$

### E. The Rate Model

The DL and UL in our work can associate with an MBS or SBS. Like prior work [3], [7], we assume the *signal-to-interference-plus-noise ratio* (SINR) of UL/DL (measured from the UE) of the candidate cells are known for a given power fraction $\rho_u$ (see Eqs. (5) - (8)). We convert the SINR to the data rate using the Shannon capacity formula, which is then used to calculate the data rate per resource unit for a given UE $u$. This conversion is described as follows.

We denote $r_{u,A,m}^{UL}$ and $r_{u,nA,m}^{UL}$ as the per-resource-unit data rate for the ABS $A$ and nABS $nA$ respectively, when the UL of UE $u$ is associated to macrocell $m$. In a similar vein, we use $r_{u,A,s}^{UL}$ and $r_{u,nA,s}^{UL}$ to denote the per-resource-unit data rate for ABS $A$ and nABS $nA$ respectively, when the UL is assigned to smallcell (e.g pico) $s$. Following this naming convention, for UE $u$, $r_{u,nA,m}^{DL}$ is the per-resource-unit data rate for nABS when its DL is associated to macrocell $m$, $r_{u,A,s}^{DL}$ and $r_{u,nA,s}^{DL}$ are the per-resource-unit data rates for ABS and nABS when its DL is assigned to smallcell $s$.

The resources units allocated to UE $u$ are denoted as $c_{u,A}^{UL}$, $c_{u,nA}^{UL}$, $c_{u,nA}^{DL}$ for MBS $m$, and $d_{u,A}^{UL}$, $d_{u,nA}^{UL}$, $d_{u,A}^{DL}$ $d_{u,nA}^{DL}$ for SBS $s$. Here $c_{u,A}^{UL}$ ($d_{u,A}^{UL}$) is the number of allocated resource for ABS from MBS $m$ (or SBS $s$) on the UL; $c_{u,nA}^{UL}$ ($d_{u,nA}^{UL}$) and $c_{u,nA}^{DL}$ ($d_{u,nA}^{DL}$) are the numbers of allocated resource units for nABSs from MBS $m$ (or SBS $s$) on the UL and DL respectively. $d_{u,A}^{DL}$ is the number of allocated resource units in ABS from SBS $s$ on the DL.

Thus, the rate of UE $u$ is the sum of the UL and DL data rates: $R(u) = R_u^{UL} + R_u^{DL}$, with $R_u^{UL}$ and $R_u^{DL}$ defined as:

$$R_u^{UL} = \begin{cases} c_{u,A}^{UL} \cdot r_{u,A,m}^{UL} + c_{u,nA}^{UL} \cdot r_{u,nA,m}^{UL}, \text{UL-MBS} \\ d_{u,A}^{UL} \cdot r_{u,A,s}^{UL} + d_{u,nA}^{UL} \cdot r_{u,nA,s}^{UL}, \text{UL-SBS} \end{cases} \tag{9}$$

$$R_u^{DL} = \begin{cases} c_{u,nA}^{DL} \cdot r_{u,nA,m}^{DL}, \text{DL-MBS} \\ d_{u,A}^{DL} \cdot r_{u,A,s}^{DL} + d_{u,nA}^{DL} \cdot r_{u,nA,s}^{DL}.\text{DL-SBS} \end{cases} \tag{10}$$

$$SI_{s,A}^{DL}(u) = \frac{\rho_u P_s^{DL} \cdot H_{u,s}}{\sum_{s\in I_s} \rho_u P_s^{DL} H_{u,s} + \sum_{u\in I_u} P_u^{UL} H_{u,u} + N_0} \quad \text{for ABS subframes}$$
$$SI_{s,nA}^{DL}(u) = \frac{\rho_u p_s^{DL} \cdot H_{u,s}}{\sum_{s\in I_s} \rho_u P_s^{DL} H_{u,s} + \sum_{m\in I_s} \rho_u P_m^{DL} H_{u,m} + \sum_{u\in I_u} P_u^{UL} H_{u,u} + N_0} \quad \text{for nABS subframes} \tag{5}$$

$$SI_{s,A}^{UL}(u) = \frac{p_u^{UL} \cdot H_{u,s}}{\sum_{s\in I_s} \rho_u P_s^{DL} H_{s,s} + \sum_{u\in I_u} P_u^{UL} H_{u,s} + N_0} \quad \text{for ABS subframes}$$
$$SI_{s,A}^{UL}(u) = \frac{p_u^{UL} \cdot H_{u,s}}{\sum_{s\in I_s} \rho_u P_s^{DL} H_{s,s} + \sum_{m\in I_s} \rho_u P_m^{DL} H_{m,s} + \sum_{u\in I_u} P_u^{UL} H_{u,s} + N_0} \quad \text{for nABS subframes} \tag{6}$$

$$SI_m^{DL}(u) = \frac{\rho_u P_m^{DL} \cdot H_{u,m}}{\sum_{s\in I_s} \rho_u P_s^{DL} H_{u,s} + \sum_{m\in I_m} \rho_u P_m^{DL} H_{u,m} + \sum_{u\in I_u} P_u^{UL} H_{u,u} + N_0} \text{for nABS subframes} \tag{7}$$

$$SI_{m,A}^{UL}(u) = \frac{p_u^{UL} \cdot H_{u,m}}{\sum_{s\in I_s} \rho_u P_s^{DL} H_{s,m} + \sum_{u\in I_u} P_u^{UL} H_{u,m} + N_0} \quad \text{for ABS subframes}$$
$$SI_{m,nA}^{UL}(u) = \frac{p_u^{UL} \cdot H_{u,m}}{\sum_{s\in I_s} \rho_u P_s^{DL} H_{s,m} + \sum_{m\in I_m} \rho_u P_m^{DL} H_{m,m} + \sum_{u\in I_u} P_u^{UL} H_{u,m} + N_0} \quad \text{for nABS subframes} \tag{8}$$

## IV. Formulation of the Optimization Problem

In the section, we first describe the optimization constraints of our problem before we formulate it.

### A. Optimization Constraints

*Interference:* For MBS-SBS interference management, the number of ABSs allocated to a smallcell must not exceed the maximize number of ABSs provided by any of its neighboring macrocells in the set $I_s$ that interfere with smallcell (see also Section III-B):

$$A_s + B_m \leq F, \forall s, m \in I_s \tag{11}$$

*Total airtime:* This ensures that the total average airtime for wireless transmission allocated to users from macrocell or smallcell is within the total available number of subframes. This is expressed as (see also Section III-E):

$$\sum_{u\in U_m} (c_{u,nA}^{UL} + c_{u,nA}^{DL}) \leq B_m, \forall m \in M \tag{12}$$

$$\sum_{u\in U_m} c_{u,A}^{UL} \leq (F - B_m), \forall m \in M \tag{13}$$

$$\sum_{u\in U_s} (d_{u,A}^{UL} + d_{u,A}^{DL}) \leq A_s, \forall s \in S \tag{14}$$

$$\sum_{u\in U_s} (d_{u,nA}^{UL} + d_{u,nA}^{DL}) \leq (F - A_s), \forall s \in S \tag{15}$$

*Valid values:* The number of allocated resource units must be non-negative integer numbers. The constraints can be formulated as:

$$A_s, B_m \in [0, 1, ..., F], \forall s \in S, m \in M \tag{16}$$

$$\nu_s \in [0, 1, ..., \nu^{max}], \forall s \in S \tag{17}$$

$$c_{u,A}^{UL}, c_{u,nA}^{UL}, c_{u,nA}^{DL} \in N^+ \tag{18}$$

$$d_{u,A}^{UL}, d_{u,nA}^{UL}, d_{u,A}^{DL}, d_{u,nA}^{DL} \in N^+ \tag{19}$$

where $N^+$ is the set of non-negative integers, and $F$ is typically set to 40 [2].

*Energy transfer:* The energy transfer optimization depends on the energy splitting for DL receive power as well as interference for the target UE. The dynamic energy splitting ratio decided by the user is limited between 0 to 1, described as:

$$0 \leq \rho_u \leq 1 \tag{20}$$

### B. Problem Formulation

Our goal for maximizing the total utility for user rates can be formulated as maximizing the sum of the outputs of the utility function, $\eta$, where the utility function is applied to the UL and DL rates of all UEs in the system. Our goal can be formulated as $\max_{\psi} \sum_u \eta(R_u)$, where $\eta(R_u) = \eta(R_u^{UL}) + \eta(R_u^{DL})$. The utility function should have the properties of being concave non-decreasing and continuously differentiable [28]. We use $ln(R_u)$ as our utility function as it can maintain proportional fairness for users [28]. Our optimization variables include $\psi = \{A_s, B_m, \nu_s, \rho_u, c_{u,A}^{UL}, c_{u,nA}^{UL}, c_{u,nA}^{DL}, d_{u,A}^{UL}, d_{u,nA}^{UL}, d_{u,A}^{DL}, d_{u,nA}^{DL}\}$, where $A_s, B_m$ represent the ABS allocation for smallcell and nABS allocation for macrocell, $\nu_s$ is the REB for smallcell, $\rho_u$ is the energy transfer for UE, $c_{u,A}^{UL}, c_{u,nA}^{UL}, c_{u,nA}^{DL}$ denote the resource allocation of UL and DL for macrocell, $d_{u,A}^{UL}, d_{u,nA}^{UL}, d_{u,A}^{DL}, d_{u,nA}^{DL}$ represent the resource allocation of UL and DL for smallcell. Using these annotations, we formulate the optimization problem (OP) as follows:

$$\max_{\psi} \sum_u ln(R_u)$$
$$s.t. (11) - (20) \tag{21}$$

The hardness of the eICIC configuration problem has been stated in [2], and we will introduce the DPT-UM-ABS with DUDe into the eICIC configuration. Due to the continuous variable for energy transform and integer variable for eICIC configuration, the formulation of our optimization problem OP is a mixed-integer program that is hard to solve in general. So, a good approximate solution can be quickly found by an efficient distributed algorithm in the later parts.

## V. Problem Conversions

We design a novel algorithm to decompose the OP defined in Section IV-B into subproblems that can be quickly solved. Specifically, we translate the OP to a general consensus optimization problem with regularization [9]. This conversation allows us to develop an efficient solution (Section VI) to solve

the UL and DL association and airtime resource allocation problems for a BS and its UEs.

### A. Global Variable Consensus with Regularization

In practice, OP will be processed by multiple agents (e.g., BSs or UEs) in parallel. However, the overhead of communications and synchronization among multiple parallel agents could be prohibitively expensive. To have a cost-effective solution, we translate the original problem to an equivalent linearly-constrained problem under the consensus formulation paradigm, defined as follows:

$$\begin{aligned} &\max_{x_m,x_s,\mathbf{z}} \sum_{m\in M} g_m(x_m) + \sum_{s\in S} g_s(x_s) + \ell(\mathbf{z}) \\ &s.t. x_m - z_m = 0, m \in M \\ &\quad x_s - z_s = 0, s \in S \\ &\quad x_s(A_s), x_m(B_m), z_s(A_s), z_m(B_m) \in [0,1,...,F] \\ &\quad z_s(v_s), x_m(v_s), x_s(v_s) \in [0,1,...,v^{max}], \forall s, m \in I_s \end{aligned} \tag{22}$$

We note that after reformulation, the problem is transformed into $M$ dimensions, i.e., $(g_m(x_m))$ and $S$ dimensions i.e.,$(g_s(x_s))$ subproblems, which has a global variable $\mathbf{z}$ and two local variables, $x_s$ and $x_m$. Meanwhile, the constraint is that all the local variables, $x_m$ and $x_s$ must agree with $\mathbf{z}$. However, each local vector only contains a small number of the global variables. Each component of each local variable corresponds to some global variable component.

*Variable settings:* The global variable $\mathbf{z}$ in our problem consists of all the ABS components to be optimized for all MBS and SBS, respectively. The local variable $x_m$ is the local copy at MBS $m$ and $x_s$ is the local copy at SBS $s$. Furthermore, any $x_i$ consists of a selection of the optimized ABS components. Then we have the local variables $x_m := \{B_m \cup v_s | \forall s \in I_m\},\ x_s := \{A_s \cup v_s\}$. So, we define $\mathbf{z} = \{z_m, z_s\},\ z_m := \{B_m \cup v_s | \forall s \in I_m\},\ z_s := \{A_s \cup v_s\}$. It is obvious that $z_m, z_s$ are the global variable's view of what the local variable $x_m, x_s$ should be.

*Optimizing MBS*: The objective function for macrocell $m$ is denoted as:

$$g_m(x_m) = \max_{\{c^{UL}_{u,A}, c^{UL}_{u,nA}, c^{DL}_{u,nA}, \rho_u\}} \sum_{u\in U_m} ln(R_u) \tag{23}$$

which is subject to:

$$\begin{aligned} &\sum_{u\in U_m} (c^{UL}_{u,nA} + c^{DL}_{u,nA}) \le B_m, \forall m \in M \\ &\sum_{u\in U_m} c^{UL}_{u,A} \le (F - B_m), \forall m \in M \\ &0 \le \rho_u \le 1 \\ &c^{UL}_{u,A}, c^{UL}_{u,nA}, c^{DL}_{u,nA} \in N^+ \end{aligned} \tag{24}$$

*Optimizing SBS:* The objective function for smallcell $s$ is denoted as:

$$g_s(x_s) = \max_{\{d^{UL}_{u,A}, d^{UL}_{u,nA}, d^{DL}_{u,A}, d^{DL}_{u,nA}, \rho_u\}} \sum_{u\in U_s} ln(R_u) \tag{25}$$

which is subject to:

$$\begin{aligned} &\sum_{u\in U_s} (d^{UL}_{u,A} + d^{DL}_{u,A}) \le A_s, \forall s \in S \\ &\sum_{u\in U_s} (d^{UL}_{u,nA} + d^{DL}_{u,nA}) \le (F - A_s), \forall s \in S \\ &0 \le \rho_u \le 1 \\ &d^{UL}_{u,A}, d^{UL}_{u,nA}, d^{DL}_{u,A}, d^{DL}_{u,nA} \in N^+ \end{aligned} \tag{26}$$

*Regularization:* The regularization function $g(z)$ for OP is checked if the DPT-UM-ABS subframes (see Figure 3) for the global variable $\mathbf{z}$ violates the interference constraint $C1$ or not. This is expressed as:

$$\ell(z) = \begin{cases} -\infty, z[F - B_m] < z[A_s], \forall (s, m \in I_s). \\ 0, otherwise, \end{cases} \tag{27}$$

where $z(A_s), z(B_m) \in [0, 1, ..., F]$.

## VI. Solving the Converted Optimization Problem

In this section, we first describe how to solve the converted optimization problem for UL/DL association and resource allocation based the ADMM algorithm [9] which is an efficient tool for distributed optimizations. We then describe how to jointly optimize UL/DL association and resource allocation and energy transfer, before analyzing the complexity of our solution.

### A. The ADMM-based Algorithm

Our consensus optimization problem can be formulated as an augmented Lagrangian dual problem [29] as:

$$L(\mathbf{x}, \mathbf{z}, \mathbf{y}) = \ell(\mathbf{z}) + \sum_{i\in P\cup M} (g_i(x_i) - y_i^T(x_i - z_i) - \frac{\lambda}{2}\|x_i - z_i\|_2^2 \tag{28}$$

This formula includes a penalty factor $\lambda > 0$ and dual variables $y_i \in \{y_m \cup y_s\}$ $(m \in M, s \in S)$. The dual variables $y_s$ has the same optimized components as $x_s$, i.e., $\Omega(y_s) = \Omega(x_s)$, which the variable $y_m$ is the same as. Note that $\|, \|_2^2$ is the Euclidean norm. The corresponding dual function is defined as:

$$J(\mathbf{y}) = \max_{\mathbf{x},\mathbf{z}} L(\mathbf{x}, \mathbf{z}, \mathbf{y}) \tag{29}$$

And the dual problem is defined as:

$$\min_{\mathbf{y}} J(\mathbf{y}) \tag{30}$$

Using this formulation, we can construct an iterative ADMM-based algorithm according to [3]. To update variables for the $n+1$ step using results of the $n$ step, we perform the following operations:

*1) $x$ is updated as following, where $x = \{x_m, x_s\}$.*

For each MBS $m \in M$, it updates $x_m$ as:

$$x_m^{n+1} = arg\max_m (g_m(x_m) - y_m^{nT}(x_m - z_m^n) - \frac{\lambda}{2}\|x_m - z_m^n\|_2^2) \tag{31}$$

where $x_m = \{x_m(B_m), x_m(v_s) | \forall s \in I_m\}$, and $g_m(x_m)$ is computed by Eq. 23 with the value $\{c^{UL}_{u,A}, c^{UL}_{u,nA}, c^{DL}_{u,nA}, \rho_u\}$.

For each SBS $s \in S$, it updates $x_s$ as:

$$x_s^{n+1} = arg\max_s (g_s(x_s) - y_s^{nT}(x_s - z_s^n) - \frac{\lambda}{2}\|x_s - z_s^n\|_2^2) \tag{32}$$

where $x_s = \{x_s(A_s), x_s(v_s)\}$, and $g_s(x_s)$ is computed by Eq. 25 with $\{d_{u,A}^{UL}, d_{u,nA}^{UL}, d_{u,A}^{DL}, d_{u,nA}^{DL}, \rho_u\}$.

*2) $y$ is updated as following, where $y = \{y_m, y_s\}$.*

For each MBS $m \in M$, the update of $y_m$ is conducted by:

$$y_m^{n+1} = y_m^n + \lambda(x_m^{n+1} - z_m^{n+1}) \tag{33}$$

For each SBS $s \in S$, the update of $y_s$ is conducted by:

$$y_s^{n+1} = y_s^n + \lambda(x_s^{n+1} - z_s^{n+1}) \tag{34}$$

*3) $z$ is updated as following, where $x = \{z_m, z_s\}$.*

For each MBS $m \in M$, the $z_m \in \mathbf{z}$ update is denoted as:

$$z_m^{n+1} = arg\max_{z_m}(\ell(\mathbf{z}) + \sum_{m \in M}(y_m^{nT} z_m - \frac{\lambda}{2}\|x_m^{n+1} - z_m\|_2^2) \tag{35}$$

where $z_m = \{z_m(B_m), z_m(v_s) | \forall s \in I_m\}$.

For each SBS $s \in S$, the $z_s \in \mathbf{z}$ update is denoted as:

$$z_s^{n+1} = arg\max_{z_s}(\ell(\mathbf{z}) + \sum_{s \in S}(y_s^{nT} z_s - \frac{\lambda}{2}\|x_s^{n+1} - z_s\|_2^2) \tag{36}$$

where $z_s = \{z_s(A_s), z_s(v_s)\}$.

The $z$ update in the REB component ($z_s[\nu_s]$) is denoted as:

$$\begin{aligned} z_s^{n+1}(\nu_s) = Int(&\frac{x_s^{n+1}[\nu_s] + \sum_{m \in I_s} x_m^{n+1}[\nu_s]}{1 + |I_s|} \\ &+ \frac{y_s^n[\nu_s] + \sum_{m \in I_s} y_m^n[\nu_s]}{\lambda(1 + |I_s|)}) \end{aligned} \tag{37}$$

where $Int(.)$ maps the input to an integer between 0 and $\nu_s^{max}$.

The $z$ update step for the DPT-UM-ABS components, i.e., $z(A_s) = \{A_s | s \in I_m\}$, is obtained by computing:

$$z^{n+1}(A_s) = arg\min_{A_s} \sum_{s \in I_m} \|z(A_s) - (x_s^{n+1}(A_s) + y_s^n(A_s)/\lambda)\|_2^2 \tag{38}$$

We note that the aforementioned steps 2 and 3 for updating $y$ and $z$ are straightforward to calculate. In the next sub-section, we discuss how to implement step 1 for updating $x_s, x_m$.

### B. Updating $x_s$ for SBS

*Basic idea:* There are three components $x_s(A_s)$ , $x_s(\nu_s)$ and $x_s(\rho_u)$ for $x_s$. For any given $x_s$, the second and third parts in Eq. 32 can be computed within a constant time, $O(1)$. Thus, Eq. 32 is solved by applying any possible $x_s$ to $g_s(x_s)$. The $x_s(A_s)$, $x_s(\nu_s)$ belong to a finite positive integer, while the $x_s(\rho_u)$ is the continuous value between 0 to 1. Therefore, we optimize alternatively the integer variable and continuous variable. The number of steps for possible $x_s$ is $(1+F)*(1+\nu_s^{max})$ (see Section III-B), if we only optimize two components in $x_s(A_s)$, $x_s(\nu_s)$. Then, we transform the non-convex problem with $x_s(\rho_u)$ for given $x_s(A_s)$, $x_s(\nu_s)$ into the convex problem based on the structure of the problem.

*DL/UL association and resource allocation:* To optimize the smallcell objective function, $g(x_s)$, in Eq. 25, we start by sorting users in $U_s^C \cup U_s^E$ according to $\epsilon_u$ (Section III-B), where $|U_s^C| = |U_s^{UL} \cup U_s^{C,DL}|$ denotes all UEs that can be associated with smallcell $s$ (including UL associations and the DL association of the center UE), and $U_s^E$ denotes all edge UEs' DL that can be associated with for smallcell $s$. We denote the $j$th UE in the sorted list as UE $j$. Then, the auxiliary function $h_s(j(v_s), d_A, d_{nA}, \rho_u)$ is defined as the maximum utility obtained by giving $d_A = A_s$ and $d_{nA} = F - A_s$ resource units in ABSs and nABSs respectively to UEs that precede UE $j$. We can then obtain:

$$g_s(x_s) = h(|U_s^C + x_s(\nu_s)|, A_s, F - A_s, \rho_u) \tag{39}$$

We can calculate $g_s(x_s)$ using divide and conquer. Starting from an empty sorted user list, i.e., $n = 0$, we have $h_s(0, d_A, d_{nA}, \rho_s) = 0$ for any $d_A$ and $d_{nA}$. We solve the problem by iteratively dividing the available resources into two parts using the $jth$ UE as the pivot and then solving resource allocation for each part individually. The Bellman equation is expressed as:

$$\begin{aligned} h(j, d_A, d_{nA}, \rho_u) = \max_{\psi_h}[&h(j-1, d_A - d_{u,A}^{*,UL} - d_{u,A}^{*,DL}, \\ &d_{nA} - d_{u,nA}^{*,UL} - d_{u,nA}^{*,DL}, \rho_u) \\ &+ ln(d_{u,A}^{UL} \cdot r_{u,A,s}^{UL} + d_{u,nA}^{UL} \cdot r_{u,nA,s}^{UL}) \\ &+ ln(d_{u,A}^{DL} \cdot r_{u,A,s}^{DL} + d_{u,nA}^{DL} \cdot r_{u,nA,s}^{DL})] \end{aligned} \tag{40}$$

Due to the problem structure for a given $\rho_u$, dynamic programming can then be used to compute $g_s(x_s(A_s), x_s(v_s))$ and $d_{u,A}^{UL}, d_{u,nA}^{UL} d_{u,A}^{DL}, d_{u,nA}^{DL}$ according to Eqs. 39 and 40.

*Energy transfer optimization:* If we determined the association and resource allocation by the dynamic programming for smallcell, we adopt the non-linear EH model for energy transfer optimization. To improve the energy efficient of IoT device, the energy transfer optimization with practical non-linear EH model is to maximize the total harvested power. Furthermore, we directly use practical $\Psi_u$ (eq. 4) to represent the harvested power at IoT device of user $u$ for simplicity. Then the energy transfer optimization can be transformed into:

$$\begin{aligned} &\max_{\rho_u} \sum_{u \in U_s} \Psi_u \\ &s.t.: 0 \le \rho_u \le 1 \end{aligned} \tag{41}$$

In order to obtain a tractable solution, the non-convex objective function can be transformed into an equivalent objective function in subtractive form [21].

$$\begin{aligned} &\max_{\rho_u, \mu_u, \beta_u} \sum_{u \in U_s} \mu_u[M_u - \beta_u(1 + exp(-a_u((1-\rho_u)P_u^{Rx} - b_u)))] \\ &s.t.: 0 \le \rho_u \le 1 \end{aligned} \tag{42}$$

where $\mu_u$, $\beta_u$ is a non-negative parameter. It is easy to prove that (42) is convex, which can be solved by standard numerical algorithms for convex programs [30].

*Joint optimization:* The first step, for an initial $\rho_u^0, u \in U_s$, we can obtain $x_s(A_s), x_s(v_s)$ and $d_{u,A}^{UL}, d_{u,nA}^{UL} d_{u,A}^{DL}, d_{u,nA}^{DL}$. If the UL/DL association and resource allocation are determined by the dynamic programming. Then, second step, the $\rho_u, u \in U_s$ is computed by the convex algorithm [29]. For the $\rho_u^{n,*}, u \in U_s$ obtained, we iterate the first step again. The first and second step is alternately iterated until the stop condition $|g_s(x_s)^{n+1} - g_s(x_s)^n| < \delta_s$ is satisfied in Algorithm 1. The choices of $\delta$ depend on the application and the iterated algorithm is implemented in SBS.

### C. Updating $x_m$ for MBS

*Basic idea:* There are three components $x_m(B_m)$, $x_m(\nu_s)|s \in I_m$ and $x_m(\rho_u)$ for $x_s$. The number of components to be optimized in local variable $x_m$ is $\Pi(x_m) = 1 + |I_m|$. However, due to the large number of possible values, we cannot simply search for an optimal value for $x_m$. Instead, we divide all UEs that can be assigned to macro $m$ into $1 + |I_m|$ groups. Group $G_0 = U_m^{UL} \cup U_m^{C,DL}$ includes the UEs whose UL is associated with macrocell $m$ ($U_m^{UL}$) as well as the center UE whose DL is associated with macrocell $m$ ( $U_m^{C,DL}$). Group $G_j = U_m^{DL} \cap U_{s_j}^{E,DL} (1 \leq j \leq |I_m|)$ are the *edge* UEs whose DL can be associated with macrocell $m$ or the $jth$ neighboring smallcell $s_j$, $s_j \in I_m$.

The component of $x_m(B_m)$ can be used for UL and DL transmission while $F - x_m(B_m)$ is only used for UL transmission. Here, the objective value in Eq. 31 is treated as the sum of the gain of all UE groups when the number of the total available resources are $F$. We also note that the optimizing components of $x_m[\nu_s]$ will only affect the UL/DL gain of one UE group at a time.

The grouping strategy allows us to reduce the search space by only enumerating a much smaller number of integer values (between 0 and $F$ – typically is 40, which is the total number of subframes in one ABS cycle [2] [3]) of $x_m(B_m)$ to maximize the objective function of Eq. 31, formulated as:

$$\begin{aligned} \max_{x_m(B_m)} \; & q_1[x_m(B_m)] - y_m^n(B_m)[x_m(B_m) - z_m^n(B_m)] \\ & -(\lambda/2)\|x_m(B_m) - z_m^n(B_m)\|_2^2 \end{aligned} \tag{43}$$

where $q_1(c)$ decides how to allocate $c$ resource units among the UE groups, i.e.,

$$q_1(c) = \sum_{j=0}^{|I_m|} q_2(j, c_j), s.t. \; 0 \leq \sum_{j=0}^{|I_m|} c_j \leq c. \tag{44}$$

where $q_2(j; c)$ is the objective value obtained from the UEs in $G_j$ with the consideration of optimized component $x_m(\nu_{s_j})$. We have $q_2(0; c) = q_r(G_0; c)$ for $j = 0$ and the following expressions for $j \neq 0$.

$$\begin{aligned} q_2(j; c) = \max_{x_m(\nu_{s_j})} & [q_r(G(j, x_m(\nu_{s_j})), c) \\ & - y_m^n(\nu_{s_j})[x_m(\nu_{s_j}) - z^n(\nu_{s_j})] \\ & - (\lambda/2)\|x_m(\nu_{s_j}) - z^n(\nu_{s_j})\|_2^2] \end{aligned} \tag{45}$$

where $G(j; x_m(\nu_{s_j})) = U_m^{DL} \cup (U_{s_j}^{E,DL}, x_m(\nu_{s_j})) \subseteq G_j$ denotes the set of UEs which are associated with macrocell $m$ in line with $x_m(\nu_{s_j})$.

Next, we define $q_r(G, c_A, c_{nA})$ to be the Bellman equation to perform resource allocation for a UE in $G$ ($u \in G$), where there are $c_A, c_{nA}$ numbers of available resource units. This is expressed as:

$$\begin{aligned} q_r(G, b) = \max_{\psi_q} & \sum_{u \in G} [ln(c_{u,A}^{UL} r_{u,A,m}^{UL} + c_{u,nA}^{UL} r_{u,nA,m}^{UL}) \\ & + ln(c_{u,nA}^{DL} r_{u,nA,m}^{DL})] \\ s.t & \sum_{u \in U_m} (c_{u,nA}^{UL} + c_{u,nA}^{DL}) \leq B_m, \forall m \in M \\ & \sum_{u \in U_m} c_{u,A}^{UL} \leq (F - B_m), \forall m \in M \end{aligned} \tag{46}$$

where $\psi_q = \{c_{u,A}^{UL}, c_{u,nA}^{UL}, c_{u,nA}^{DL}\}$.

*DL/UL association and resource allocation:* To compute the resource allocation function, $q_1$, $q_2$, and $q_r$, for a given UE group $G_j$, we turn again to divide and conquer (see Section VI-B). We start by sorting the UEs in descending order of $\epsilon_u$, the RSRP difference in Section III-B). We denote the $j$th UE in the sorted list as UE $j$. We then apply a similar divide and conquer strategy described in Section VI-B to macrocells. The utility function used for allocation is $G_j(j, c_A, c_{nA})$, where $c_A = F - B_m$ and $c_{nA} = B_m$ are the resource units in ABSs and nABSs respectively given to UEs that precede UE $j$. This process is modeled as:

$$\begin{aligned} G_j(j, c_A, c_{nA}) = \max_{\psi_G} & [G_j(j-1, c_A - c_{u,A}^{*,UL}, c_{nA} - c_{u,nA}^{*,UL} - c_{u,nA}^{*,DL}) \\ & + ln(c_{u,A}^{UL} r_{u,A,m}^{UL} + c_{u,nA}^{UL} r_{u,nA,m}^{UL}) \\ & + ln(c_{u,nA}^{DL} r_{u,nA,m}^{DL})] \end{aligned} \tag{47}$$

where $\psi_G = \{c_{u,A}^{UL}, c_{u,nA}^{UL}, c_{u,nA}^{DL}\}$.

For Eq. 45, we have $q_2(0; c) = G_0(|G_0|, c_A, c_{nA})$ for the macro center UE group of the DL as well as UEs whose UL is associated with macro $G_0$. For a given UE group $G_j$ where $j \neq 0$, the components of $x_m(\nu_{s_j})$ to be optimized are mapped into two parts of the sorted list, using $G_j$ as the partitioning pivot. We then assign the first and second parts to a macro and a small cells respectively by applying $q_2$. Specifically, $q_2$ can be expressed as:

$$\begin{aligned} q_2(j; c) = \max_{x_m(\nu_{s_j})} & ((G_j[(x_m(\nu_{s_j}), c_A, c_n A] \\ & - y_m^n(v_{s_j})(x_m(\nu_{s_j}) - z^n(\nu_{s_j}))] \\ & - (\lambda/2)\|x_m(\nu_{s_j}) - z^n(\nu_{s_j})\|_2^2) \end{aligned} \tag{48}$$

In the same vein, we can define an auxiliary function and use it to solve $q_1(c)$ of Eq. 44. The auxiliary function, $V(j; c)$, is defined as the maximum value obtained by giving the first $j$ UE groups $c$ available resources. As a result, we have:

$$q_1(c) = V(|I_m| + 1, c) \tag{49}$$

Like our previous divide-and-conquer strategy, we iteratively solve $q_1$. We start by computing $V(0; c)$, where we have $V(0; c) = q_2(0; c)$ for any $c$. We then use UE $j$ to divide the sorted list of UEs into two parts, and solve each part individually. This process is formulated as:

$$V(j; c) = \max_{0 \leq c^* \leq c} [V(j-1; c - c^*) + q_2(j, c^*)] \tag{50}$$

If we get all possible values of $q_1(c)$, we can compute Eq. 43 through enumerating all possible values (typically no more than 40 values) of $x_m(B_m)$ and $F - x_m(B_m)$.

Finally, the results of resource allocation for function $q_r(.)$ are solved with dynamic programming based algorithm by implementing the iterative steps of Eqs. 49 and 50.

*Energy transfer optimization:* Similar to the VI-B, if we determined the association and resource allocation by the dynamic programming for macrocell, the energy transfer optimization with non-linear EH model is to maximize the total harvested power and can be formulated into:

$$\begin{aligned} & \max_{\rho_u} \sum_{u \in U_m} \Psi_u \\ & s.t. : 0 \leq \rho_u \leq 1 \end{aligned} \tag{51}$$

The non-convex objective function can also be transformed into an equivalent function [21].

$$\max_{\rho_u,\mu_u,\beta_u} \sum_{u\in U_m} \mu_u[M_u - \beta_u(1+exp(-a_u((1-\rho_u)P_u^{Rx} - b_u)))] \\ s.t.: 0 \le \rho_u \le 1 \tag{52}$$

where $\mu_u$, $\beta_u$ is a non-negative parameter. It is easy to prove that (42) is convex, which can be solved by standard numerical algorithms for convex programs [30].

*Joint optimization:* We solve the joint optimization problem using a two-step iterative algorithm that runs on an MBS in Algorithm 1. In the first step, for an initial $\rho_u^0, u \in U_m$, we obtain $x_m(B_s), x_m(v_s)$ and $c_{u,A}^{UL}, c_{u,nA}^{UL} c_{u,nA}^{DL}$. Here, the DL/UL association and resource allocation for macrocell users are determined by the dynamic programming solution described in Eqs.49 and 50. In the second step, we compute $\rho_u, u \in U_m$ using the convex algorithm [29]. To obtain the optimal $\rho_u^{n,*}, u \in U_m$, we iterate the first step. Then, the first and second steps are alternately iterated until the stop condition, $|g_m(x_m)^{n+1} - g_m(x_m)^n| < \delta_m$, is met, where $\delta_m$ is a configurable parameter.

### D. Complexity Analysis

The overhead of our approach mainly comes from determining the smallcell and macrocell associations, corresponding to the computation of $g_s(x_s)$ (Section VI-B) and $g_m(x_m)$ (Section VI-C), respectively. The energy transform $\rho_u$ is obtained by convex algorithm, of which the complexity is common in polynomial time between $\sqrt{2|U|}$ to $2|U|$, where $|U|$ is the number of users [29]. The complexity of joint optimization mainly depends on the DL/UL association and resource allocation in a SBS or MBS.

*SBS DL/UL association and resource allocation:* The initial step for computing $g_s(x_s)$ is to calculate $h(j, d_A, d_{nA}, \rho_u)$. The time complexity for this is $O(|U_s^{UL} \cup U_s^{DL}|F^4) < O(2|U_s|F^4)$. Once $g_s(x_s)$ is obtained, we can compute the objective result for every possible $x_s$ in Eq. 32 within constant time, i.e., $O(1)$. As the number of possible values of $x_s$ is $(1+F)(1+|U_s^E|)$, the time complexity of each $x$ update for smallcell $s$ is $O(F|U_s^E|)$.

*MBS DL/UL association and resource allocation:* The time complexity in the initial step for obtaining all the possible values for utility function $G_j(j, c_A, c_{nA})$ is $O(|U_m^{DL} + U_m^{UL}|F^2) < O(2|U_m|F^2)$. Thus, the time complexity for every $x$ update step for macrocell $m$ is $O(|I_m|(U_m^{EM,DL} + U_m^{UL})F + |I_m|F^2 + F) = O(|I_m|F(U_m^{EM,DL} + U_m^{UL} + F)) < O(2SF|U_m| + SF^2))$, where $U_m^{EM,DL}$ is the maximum number of edge UEs whose DL can be associated with one of the neighboring macrocells.

We can note that the time complexity is linear with the number of users, and the maximum exponent of $F$ is 4. Moreover, $F$ is typically 40. In general, $|U_m| < |U_s| < |U|$, where $|U|$ is the number of IoT devices.

### E. Our proposed Algorithm and Practical Implementation

The proposed ADMM based algorithm is to coordinate the solutions from local subproblems on MBS and SBS to find a solution to the global problem for the whole network. The local REB, ABS adaptation and UL/DL association and resource allocation are performed in MBS and SBS, and then global consensus variable $z$ is used to coordination among local solutions for the upper layer, as is shown in Algorithm 1.

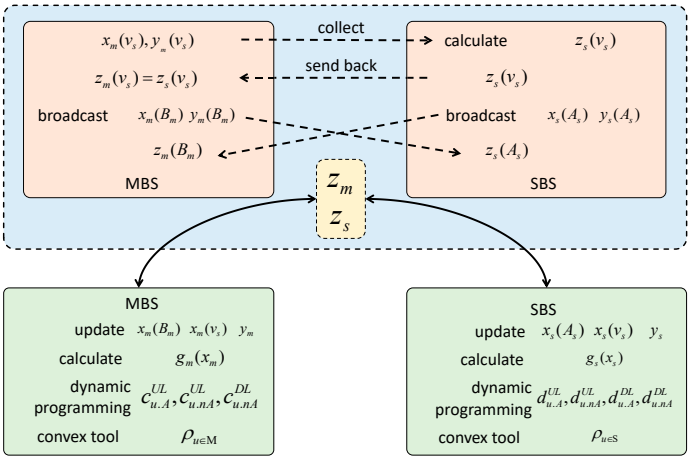


Figure 4. Practical implementation of the proposed joint optimization.

**Algorithm 1** Joint optimization of DL/UL association, resource allocation and energy transfer.

1: *Initialize*:
To take the channel gain $H_{u,BS}$ and $H_{BS,BS}$, $BS \in \{m, s\}$;
To compute the signal-to-interference-plus-noise ratio (SINR) of UL/DL by Eqs. (5) - (8);
To obtain the rate UL/DL of UE by Eqs. (9)-(10).
2: *Joint optimization*:
*Repeat* Update $x_m$, $x_s$, $y_m$, $y_s$;
Calculate $z_s(v_s)$, $g_m(x_m)$ $g_s(x_s)$;
DL/UL association and resource allocation by dynamic programme: Eqs. (39) and (40) for SBS, Eqs. (49) and (50) for MBS;
To solve energy transfer $\rho_u$ with Eqs. (42) and (52) by the convex algorithm [30] ;
*Until* $(|g_m(x_m)^{n+1} - g_m(x_m)^n| < \delta_m)$.

Our algorithm is based on the alternating direction method of multipliers (ADMM) in which the solutions to local subproblems on each MBS and SBS are coordinated to find a solution to the global problem for the whole network. If it is carried out in central manner, which can be easily implemented in MBS. We discuss the distributed manner for $z$ update, which is shown in Figure.4. $x_m(B_m)$, $x_m(v_s)$, $y_m$ are updated in MBS, and the $g_m(x_m)$ is calculated by Eq. 23. UL/DL association and resource allocation $c_{u,A}^{UL}, c_{u,nA}^{UL}, c_{u,nA}^{DL}$ are obtained by dynamic programme with Eqs. 49 and 50 in MBS. The energy transfer $\rho_{u\in M}$ of user accessing to MBS is solved by convex tool [30]. $x_s(A_s)$, $x_s(v_s)$, $y_s$ are updated in SBS, and the is calculated by Eq. 25. UL/DL association and resource allocation $d_{u,A}^{UL}, d_{u,nA}^{UL}, d_{u,A}^{DL}, d_{u,nA}^{DL}$ are obtained by dynamic programme with Eqs. 39 and 40 in SBS. The

Table II
SIMULATION SETUP FOR BASE STATIONS

| Parameter | Value | Parameter | Value |
|---|---|---|---|
| Tx power of macrocells | 46dBm | Tx power of smallcells | 30dBm |
| Carrier frequency | 2GHz | Thermal noise power | -174dBm/Hz |
| Path-loss of macrocells | 28.3+22.0$log_{10}l, lkm$ | Path-loss of smallcells | 30.5+36.7$log_{10}l, lkm$ |
| $F$ frame | 40 | Bandwidth | 1.4MHz |

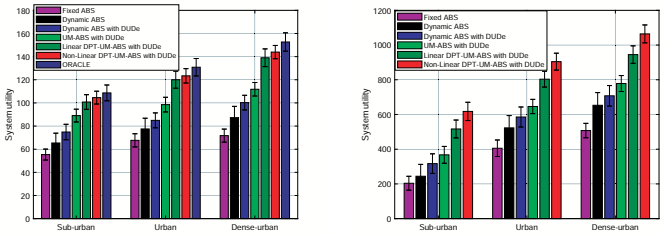


(a) *Sparse* (b) *Dense*

Figure 5. The achieved system utility under the *sparse* (a) and *dense* (b) smallcell densities.

energy transfer $\rho_{u\in S}$ of user accessing to SBS are also solved by convex method [30]. The $z$ update is responsible to find a solution to the global problem for the whole network among local solutions. The SBS collects the values $x_m(v_s), y_m(v_s)$ of from it suffered interference from MBS $z_m(v_s) = z_s(v_s)$. Then the SBS computes the by Eq. 36 and sends back to the MBS $x_m(B_m), y_m(B_m)$ . For $z$ update of ABS, MBS broadcasts $x_m(B_m)$, $y_m(B_m)$ and SBS broadcasts $x_s(A_s)$, $y_s(A_s)$, then MBS and SBS compute $z_m(B_m)$,$z_s(A_s)$ by Eqs. 35 and 36.

## VII. PERFORMANCE EVALUATION

### A. Evaluation Methodology

*Simulation setup:* We evaluate our approach via Matlab simulations. Table II lists the BS parameters used in the simulation, which are chosen according to 3GPP [31] and prior work [3] [4] for enhanced MTC (eMTC) [32]. We consider three typical deployment scenarios of different user densities, *sub-urban*, *urban* and *dense-urban*, which respectively have 250, 550, and 950 IoT devices per $km^2$. In this work, the utility function for a user $i$, $Util(r_i)$ (see Section IV-B), is set to $ln(r_i)$ where $r_i$ is the total rate of the UL and DL. However, other utility functions can also be used. We set the macrocell density to be 5 cells / $km^2$. We consider two types of smallcell densities, *sparse* (100 smallcells/$km^2$) where we can compare to the optimal performance found by exhaustive search, and *dense* (300 smallcells/$km^2$) which is a typical scenario. Finally, the locations of the small cells and users follow a uniform distribution in the simulation.

*Competitive schemes:* We compare our approach to the following alternative schemes:

- *Fixed ABS*: This strategy uses the fixed eICIC configuration that gives the best averaged performance across UEs in our evaluation scenarios. It equally splits the time between the UL and DL of a BS, and sets the ABS to $\frac{5}{40}F$, $\frac{10}{40}F$, $\frac{15}{40}F$ for each macrocell and the REB to 5dB, 10dB, 15dB for each smallcell [5] [6]. The Fixed ABS is obtained by the three (ABS, REB) combinations: ($\frac{5}{40}F$, 5 dB),($\frac{10}{40}F$, 10 dB), ($\frac{15}{40}F$, 15 dB). The UL and DL of a UE are associated with the same BS based on the RSRP of DL.
- *Dynamic ABS*: The dynamic ABS configuration of eICIC parameters is to allocate ABS between macrocells and smallcells, and to determine the flexible users association rules with REB [2] [3]. The time of UL and DL are split equally. The UL and DL of a UE are associated with the same BS based on the association of DL.
- *Dynamic ABS with DUDe*: This is the dynamic ABS with DUDe joint optimization approach for UE associations under dynamic TDD, and it assumes the UL and DL can be splitting to the different BS. But, it does not consider the UM-ABS and SWIPT for UL/DL [4]. The $\alpha$ is set to 1 so as to optimize the user throughout within $ln$ function [4] [28].
- *UM-ABS with DUDe*: This is UM-ABS with DUDe, which exploits the UL transmission for macrocells in ABSs referred to UM-ABS. The UM-ABS and DL/UL Decoupling (DUDe) are formulated as an optimization problem for dynamic eICIC configuration in HetNets, which doesn't consider the SWIPT [7].
- *Linear DPT-UM-ABS with DUDe*: Under the linear EH models of IoT device, the jointly identify the opportunity for power energy transfer of DL during nABS (DPT-nABS) and UM-ABS with DUDe is to optimize dynamic eICIC configuration.
- *Non-Linear DPT-UM-ABS with DUDe*: Under the non-linear EH models of IoT device, we jointly identify DPT-UM-ABS with DUDe to optimize dynamic eICIC configuration.
- *ORACLE*: The best-possible performance found by exhaustive positively trying all available configurations. It gives the theoretical perfect solution, which is used to quantify how close a schemes performance is to the up-bound.

*Evaluation criteria:* We use three metrics: (1) the system utility (a widely used metric for network capacity [3]), defined as $ln(R)$ (where $R$ is the total rate of UL and DL); (2) the UL, DL and overall rates, measured as bits/s/Hz; and (3) the proportional fairness, evaluated using the Jain's fairness index [28]. All the three metrics are higher is better metrics. Furthermore, because the user and cell are randomly generated, we run each simulation scenario 100 times. We then report the *geometric mean* performance and *variances* across the 100 runs to make sure our results are robust.

### B. Overall System Performance

*Sparse smallcell density:* Figure 5(a) reports the system utility achieved by all considered schemes under different user densities and the *sparse* smallcell density. The min-max bars show the range of performance across 100 simulation runs. Compared with the best-averaged Fixed ABS configuration, Dynamic ABS outperforms about 28.4% benefit by solving a ABS configuration and REB optimization problem, because

the optimal ABS received by each smallcell and the associated bias can be obtained by using Dynamic ABS algorithm. Due to the UL and DL be splitting of the same user between different BSs, Dynamic ABS with DUDe can improve the about 17.6% average performance gain than the Dynamic ABS. Further, by exploiting UL transmissions during macrocell ABSs (UM-ABS), UM-ABS with DUDe can improve average system performance gain average 18.3% compared with Dynamic ABS with DUDe. Compared to UM-ABS with DUDe, our proposed Non-Linear and Linear DPT-UM-ABS with DUDe can improve the system performance gain 24.2% and 20.2% and since we jointly identify the opportunity for energy transfer during nABS and UM-ABS with DUDe to optimize dynamic eICIC configuration in dense IoT HetNets. The ORACLE is an upper bound to the optimal solution of DTP-UM-ABS in sparse smallcell density i.e.,small-scale problem, we can obtain the gap by comparing our approach produced by the ADMM-based scheme. By contrast, our approach outperforms all alternative schemes, delivering on average, 94% (up to 96%) of the ORACLE performance. We also check results of individual simulation runs and can confirm that our approach outperforms other schemes in each run. Therefore, our approach gives the best and most reliable performance.

*Dense smallcell density:* Figure 5(b) compares the achieved system utilities across evaluation schemes. Note that for this scenario, we are unable to use exhaustive search to find the ORACLE performance due to the massive optimization space. Nonetheless, our approach consistently outperforms all other schemes across user density settings. Our proposed Linear DPT-UM-ABS with DUDe scheme can improve the network performance gain average by 26.4%, 40.7%, 59.5% and 103%, compared to UM-ABS with DUDe, Dynamic ABS with DUDe, Dynamic ABS and Fixed ABS respectively. It gives, on average, over 20% of improvement on system utility when compared to the second-best method, UM-ABS with DUDe. Furthermore, the proposed Non-Linear DPT-UM-ABS with DUDe can further improve the system performance gain 14.2% compared with the Linear DPT-UM-ABS with DUDe. The reasons is that the linear scheme does not utilize the system resources efficiently since it causes saturation at some IoT devices and underutilization at others. By jointly considering a larger set of optimization parameters in a dense HetNet, our approach leads to the best performance.

### C. User Experience

Figure 6 shows the cumulative distribution function (CDF) for the user-received DL, UL and total rates under the dense-urban user density and dense smallcell setting. The y-axis shows the percentage of users (between 0 and 1) who have a rate that is no less than a given rate on the x-axis. In general, the lower a curve as the scheme has, the better the user experience it provides. The Fixed ABS scheme delivers poor performance as about 85.5% of the users have a rate that is less than 1/bit/s/Hz. This is because a fixed strategy achieves lower performance for many user-cell associations and often overloads the cells. For DL, our proposed Non-Linear and Linear DPT-UM-ABS achieves almost similar performance as Dynamic ABS with DUDe and UM-ABS with DUDe. Considering that Dynamic ABS with DUDe and UM-ABS with DUDe does not split the DL power for energy transfer, this means that our proposed DPT-UM-ABS with DUDe does not compromise the user experience on UL transmissions. For UL, our proposed Non-Linear and Linear DPT-UM-ABS delivers better performance over all other schemes with more users obtaining a higher rate. Depending on the scheme to compare against, the improvement can due to either the exploitation of the macrocell ABS for UL transmissions, stronger UL transmission power (by using harvested energy), and a combination of both. Due to the further improved UL performance with Non-linear energy harvest model, the Non-Linear DPT-UM-ABS gives the best overall rates which translate to the shortest user-perceived delay time.

### D. Proportional-user Fairness

Figure 7 shows the Jain's fairness index (taking a value between 0 and 1) for the DL, UL and overall rates under the dense-urban setting. For a given network setting, Jain's index can be used to evaluate the degree of fairness, and a larger Jain's index corresponds to a more fair allocation [33]. It is observed that our approach consistently outperforms all other approaches across smallcell settings from Figure 7. We also observe that the index drops as the smallcell density increases. This is expected because when the number of available cells for associations goes up, there will be more room to give some users a higher bandwidth in order to maximize the overall system capacity. Nonetheless, our approach maintains the highest proportional-user fairness compared to other approaches.

### E. Computational Cost

We now compare the computational cost between RELAX-ROUND [2] [7] and our scheme because of both first translate problem and then find a solution to the converted problem space. This RELAX-ROUND first relaxes the problem constraints and then rounds up the approximated solutions to find a feasible solution [2] [7]. Figure 8 shows the number of iteration counts and simulation running time respectively for RELAX-ROUND and our approach under the dense-urban user setting. The min-max bars show the variations across simulation runs. As expected, the overhead for the solver increases as the smallcell density increases. However, our approach can find a solution to several magnitude orders faster than RELAX-ROUND. Therefore, our approach is faster and more scalable to larger networks. Note that the simulation running time can be significantly reduced by using parallel specialized hardware (e.g., FPGAs and DSPs), for which we expect a solution can be found within milliseconds in practice using our approach.

## VIII. Conclusions

This paper has presented a novel approach to enhance the capacity of dense IoT HetNets. Our approach leverages an existing interference coordination protocol to combine practical non-linear energy harvest model for SWIPT in the

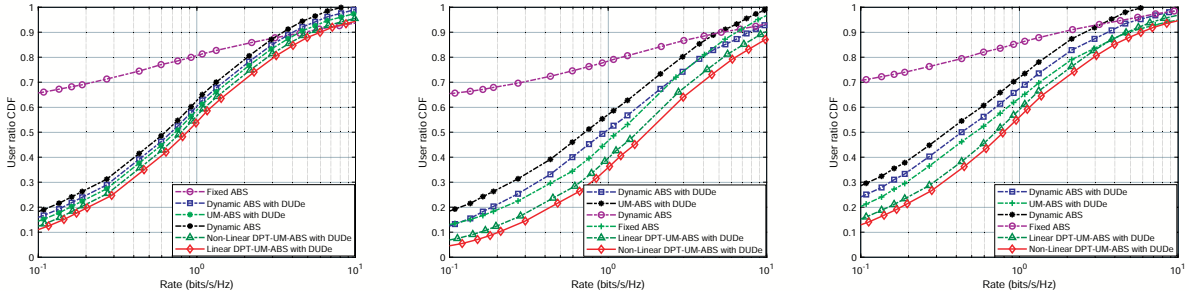


(a) CDF of the DL rate (b) CDF of the UL rate (c) CDF of the total (UL + DL) rate

Figure 6. The CDFs of DL, UL and total rates under the dense-urban user setting. There are more users having a higher rate using our approach.

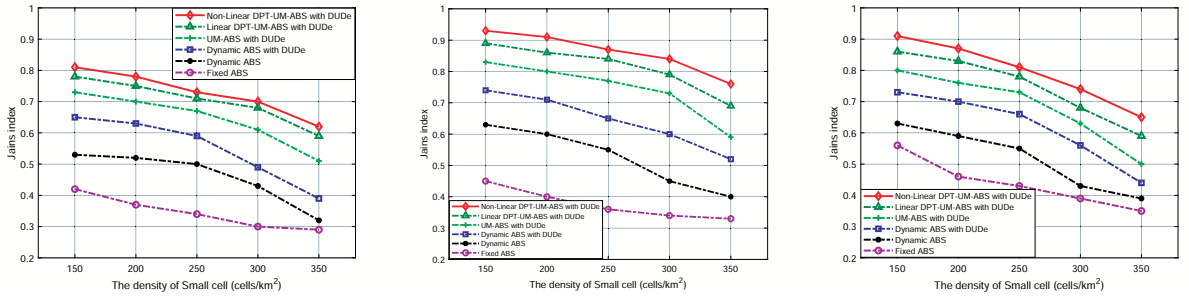


(a) The Jain's index of the DL rate (b) The Jain's index of the UL rate (c) The Jain's index of the total rate

Figure 7. The Jain's index of the UL, DL and total (DL + UL) rates under the dense-urban user setting.

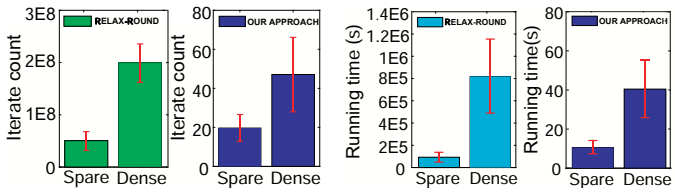


(a) *Iterate count* (b) *Running time*

Figure 8. Comparing the number of iterations (a) and simulation running time (b) for RELAX-ROUND and our approach for problem solving.

DL transmission. It further utilizes the silent DL transmission windows of macrocells to identify opportunities for additional UL transmissions. Then, we jointly optimize UL/DL associations, resource allocation and DL energy transfer because doing so can significantly boost the performance. To tackle the huge problem space, we map the highly complex co-optimization problem into a space where a solution can be quickly derived. Compared to state-of-the-arts, our approach improves the system utility, delivers a higher standard in user fairness and rate experience, and can solve the program in a fast and scalable way.

## REFERENCES


[1] S. K. Sharma and X. Wang, "Toward massive machine type communications in ultra-dense cellular IoT networks: Current issues and machine learning-assisted solutions," *IEEE Commun. Surv. Tut.*, vol. 22, no. 1, pp. 426–471, 2020.

[2] S. Deb, P. Monogioudis, J. Miernik, and J. P. Seymour, "Algorithms for enhanced inter-cell interference coordination (eICIC) in LTE HetNets," *IEEE/ACM Trans. Netw.*, vol. 22, no. 1, pp. 137–150, 2014.

[3] H. Zhou, Y. Ji, X. Wang, and S. Yamada, "eICIC configuration algorithm with service scalability in heterogeneous cellular networks," *IEEE/ACM Trans. Netw.*, vol. 25, no. 1, pp. 520–535, 2017.

[4] N. Sapountzis, T. Spyropoulos, N. Nikaein, and U. Salim, "Joint optimization of user association and dynamic TDD for ultra-dense networks," in *IEEE INFOCOM 2018*, pp. 2681–2689, Apr. 2018.

[5] D. Lopez-Perez, I. Guvenc, G. de la Roche, M. Kountouris, T. Q. S. Quek, and J. Zhang, "Enhanced intercell interference coordination challenges in heterogeneous networks," *IEEE Wireless Commun.*, vol. 18, no. 3, pp. 22–30, 2011.

[6] M. I. Kamel and K. M. F. Elsayed, "Performance evaluation of a coordinated time-domain eICIC framework based on ABSF in heterogeneous LTE-Advanced networks," *in 2012 IEEE Global Communications Conference (GLOBECOM)*, pp. 5326–5331, Apr. 2012.

[7] J. Zheng, J. Li, N. Wang, and X. Yang, "Joint load balancing of downlink and uplink for eICIC in heterogeneous network," *IEEE Trans. Veh. Technol.*, vol. 66, no. 7, pp. 6388–6398, 2017.

[8] X. Chen, Y. Liu, L. X. Cai, Z. Chen, and D. Zhang, "Resource allocation for wireless cooperative IoT network with energy harvesting," *IEEE Trans. Wireless Commun.*, vol. 19, no. 7, pp. 4879–4893, 2020.

[9] S. Boyd, N. Parikh, E. Chu, B. Peleato, and J. Eckstein, "Distributed optimization and statistical learning via the alternating direction method of multipliers," *Foundations and Trends in Machine learning*, 2011.

[10] Z. Shen, A. Khoryaev, E. Eriksson, and X. Pan, "Dynamic uplink-downlink configuration and interference management in TD-LTE," *IEEE Commun. Mag.*, vol. 50, no. 11, pp. 51–59, 2012.

[11] B. Zhang, L. Wang, and Z. Han, "Contracts for joint downlink and uplink traffic offloading with asymmetric information," *IEEE J. Sel. Areas Commun.*, vol. 38, no. 4, pp. 723–735, 2020.

[12] B. Lahad, M. Ibrahim, S. Lahoud, K. Khawam, and S. Martin, "Joint modeling of TDD and decoupled uplink/downlink access in 5G hetnets with multiple small cells deployment," *IEEE Trans. Mob. Comput.*, pp. 1–1, 2020.

[13] M. Singhal, T. Seyfi, and A. E. Gamal, "Joint uplink-downlink cooperative interference management with flexible cell associations," *IEEE Trans. Commun.*, vol. 68, no. 9, pp. 5420–5434, 2020.

[14] K. Sun, J. Wu, W. Huang, H. Zhang, H. Hsieh, and V. C. M. Leung, "Uplink performance improvement for downlink-uplink decoupled hetnets with non-uniform user distribution," *IEEE Trans. Veh. Technol.*, vol. 69, no. 7, pp. 7518–7530, 2020.

[15] Q. Yao, T. Q. S. Quek, A. Huang, and H. Shan, "Joint downlink and uplink energy minimization in WET-enabled networks," *IEEE Trans. Wirel. Commun.*, vol. 16, no. 10, pp. 6751–6765, 2017.

[16] A. Celik, R. M. Radaydeh, F. S. Al-Qahtani, and M. Alouini, "Resource allocation and interference management for D2D-Enabled DL/UL decoupled het-nets," *IEEE Access*, vol. 5, pp. 22735–22749, 2017.

[17] H. Boostanimehr and V. K. Bhargava, "Joint downlink and uplink aware cell association in hetnets with QoS provisioning," *IEEE Trans. Wirel. Commun.*, vol. 14, no. 10, pp. 5388–5401, 2015.

[18] P. D. Diamantoulakis, K. N. Pappi, G. K. Karagiannidis, H. Xing, and A. Nallanathan, "Joint downlink/uplink design for wireless powered networks with interference," *IEEE Access*, vol. 5, pp. 1534–1547, 2017.

[19] M. A. Kishk and H. S. Dhillon, "Joint uplink and downlink coverage analysis of cellular-based RF-powered IoT network," *IEEE Trans. Green Commun. Netw.*, vol. 2, no. 2, pp. 446–459, 2018.

[20] J. Li, X. Wang, Z. Li, H. Wang, and L. Li, "Energy efficiency optimization based on eICIC for wireless heterogeneous networks," *IEEE Internet Things J.*, vol. 6, no. 6, pp. 10166–10176, 2019.

[21] E. Boshkovska, D. W. K. Ng, N. Zlatanov, and R. Schober, "Practical non-linear energy harvesting model and resource allocation for swipt systems," *IEEE Commun. Lett.*, vol. 19, no. 12, pp. 2082–2085, 2015.

[22] B. Clerckx, R. Zhang, R. Schober, D. W. K. Ng, D. I. Kim, and H. V. Poor, "Fundamentals of wireless information and power transfer: From RF energy harvester models to signal and system designs," *IEEE J. Sel. Areas Commun.*, vol. 37, no. 1, pp. 4–33, 2019.

[23] H. Zhang, M. Feng, K. Long, G. K. Karagiannidis, V. C. M. Leung, and H. V. Poor, "Energy efficient resource management in SWIPT enabled heterogeneous networks with NOMA," *IEEE Trans. on Wireless Commun.*, vol. 19, no. 2, pp. 835–845, 2020.

[24] H. Zhang, J. Zhang, and K. Long, "Energy efficiency optimization for NOMA UAV network with imperfect CSI," *IEEE J. Sel. Areas Commun.*, vol. 38, no. 12, pp. 2798–2809, 2020.

[25] M. Hua, Q. Wu, D. W. K. Ng, J. Zhao, and L. Yang, "Intelligent reflecting surface-aided joint processing coordinated multipoint transmission," *IEEE Trans. on Commun.*, pp. 1–1, 2020.

[26] C. Guo, W. He, and G. Y. Li, "Optimal fairness-aware resource supply and demand management for mobile edge computing," *IEEE Wireless Communications Letters*, pp. 1–1, 2020.

[27] F. Boccardi, J. G. Andrews, H. Elshaer, M. Dohler, S. Parkvall, P. Popovski, and S. Singh, "Why to decouple the uplink and downlink in cellular networks and how to do it," *IEEE Commun. Mag.*, vol. 54, no. 3, pp. 110–117, 2016.

[28] C. Guo, Y. Zhang, M. Sheng, X. Wang, and Y. Li, "$\alpha$-fair power allocation in spectrum-sharing networks," *IEEE Trans. Veh. Technol*, vol. 65, no. 5, pp. 3771–3777, 2016.

[29] S. Boyd and L. Vandenberghe, *Convex Optimization*. Cambridge University Press, 2004.

[30] M. Grant and S. Boyd, "CVX: MATLAB software for disciplined convex programming," *http://cvxr.com/cvx*, Sep. 2013.

[31] 3GPP, "Ts 36.300, release 13," *version 13.2.0*, 2016.

[32] C. Hsu, K. Das, and L. Jorguseski, "Multi-RAT random access scheme utilising combined licensed and unlicensed spectrum for massive machine-type communications," *2020 IEEE 91st VTC2020-Spring*, pp. 1–7, 2020.

[33] C. Guo, B. Liao, L. Huang, X. Lin, and J. Zhang, "On convexity of fairness-aware energy-efficient power allocation in spectrum-sharing networks," *IEEE Commun. Lett.*, vol. 20, no. 3, pp. 534–537, 2016.


**Jie Zheng** is currently an associate professor in the information science and technology institute at Northwest University, Xi'an, China. He received the B.Sc degree in Communications Engineering from Nanchang University in 2008 and Ph.D. degree in the Department of Telecommunications Engineering at Xidian University,China in 2014. He serves as a PC member of Globecom 2020,2021. He servers as a publication chair of IoTaaS 2020. He research interests include energy-efficient transmission, wireless resource allocation, and edge intelligence.

**Ling Gao** received his BS degree in Computer Science from Hunan University in 1985 and his MS degree in Computer Science from Northwest University in 1988. In 2005, he received PhD degree in Computer Science from Xi'an Jiaotong University, Xi'an, China. His research include Network Security and Management, Embedded Internet Service and so on. Prof. Gao was a director of China Higher Educational Information Academy, the chairman of China Computer Federation Network and Data Communications Technical Committee, a member of IEEE, and a CAET director.

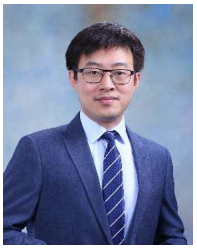

**Haijun Zhang** (M'13-SM'17) is currently a Full Professor and Associate Dean at University of Science and Technology Beijing, China. He was a Postdoctoral Research Fellow in Department of Electrical and Computer Engineering, the University of British Columbia (UBC), Canada. He serves/served as Track Co-Chair of WCNC 2020, Symposium Chair of Globecom'19, TPC Co-Chair of INFOCOM 2018 Workshop on Integrating Edge Computing, Caching, and Offloading in Next Generation Networks, and General Co-Chair of GameNets'16. He serves as an Editor of IEEE Transactions on Communications, IEEE Transactions on Network Science and Engineering, and IEEE Transactions on Vehicular Technology. He received the IEEE CSIM Technical Committee Best Journal Paper Award in 2018, IEEE ComSoc Young Author Best Paper Award in 2017, and IEEE ComSoc Asia-Pacific Best Young Researcher Award in 2019.

**Dusit Niyato** (M'09-SM'15-F'17) is currently a professor in the School of Computer Science and Engineering, at Nanyang Technological University, Singapore. He received B.Eng. from King Mongkuts Institute of Technology Ladkrabang (KMITL), Thailand in 1999 and Ph.D. in Electrical and Computer Engineering from the University of Manitoba, Canada in 2008. His research interests are in the areas of Internet of Things (IoT), machine learning, and incentive mechanism design.

**Jie Ren** is currently an assistant professor in Shaanxi Normal University, Xian, China. He serves as a PC member of IJCAI 2021 and SocialCom 2020. He servers as a session chair of UIC 2018.

**Hai Wang** was born in 1977, Ph.D. He is currently an associate professor at information science and technology institute at Northwest University, Xian, China. His research interests include mobile-net work management, edge computing and machine learning.

**Hongbo Guo** received the Ph.D. degree in Computer Applications Technology from Northwest University, China. He is currently an Associate Professor with the Department of Information and Communication Engineering, the School of Information Sciences and Technology, Northwest University. His research was sponsored by several the National Science Foundations. He has published around 30 research articles in international conferences and journals. His research interests are in the area of image processing, and edge computing.

**Zheng Wang** is currently an associate professor with the University of Leeds. His research cut across the boundaries of parallel program optimisation, systems security, and applied machine learning. He received four best paper awards for his work on machine learning-based compiler optimisation (PACT '10, CGO '17, PACT '17, and CGO '19).